Updated July 31st, 2005

Chapter IV Quarter-Wavelength Antenna

Contents

4.1 Metal monopole at 400 MHz

The monopole antenna (cf. [1]) is the simplest quarter-wavelength single-band omnidirectional antenna with a relatively large bandwidth – up to 10% or so. The monopole is fed by a coaxial cable and does not require a balun transformer. However, the monopole performance is affected by the size of the ground plane, which ideally should be large. The dependence of the input impedance on monopole thickness is less significant. The scholarly papers on the monopole on a finite ground plane include Refs. [2, 3].

A thin monopole antenna is a numerically challenging example for a surface patch code since a fine surface mesh of the entire monopole length is necessary in order to obtain accurate results. This is in contrast to the patch antenna where finer meshing of the feeding column has little influence on the antenna behavior.

a. Geometry

This example describes a monopole antenna of height 180 mm on a small ground plane – a square metal plate with a size of 400 mm. The antenna geometry is shown in Fig. 4.1.

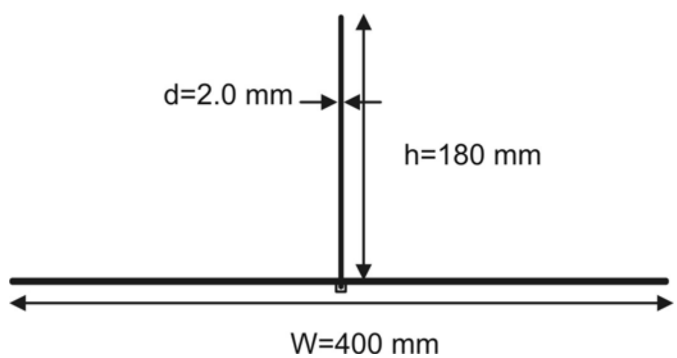

Fig. 4.1. Monopole antenna.

The antenna has the following features:

1. The monopole has an omnidirectional radiation pattern, vertical polarization, and a relatively large bandwidth. However, it cannot be matched to 50 Ω automatically, in contrast to the dipole, since the monopole impedance is twice as small as that of the dipole.
2. The monopole is a thin cylindrical column with a diameter of d=2.0 mm. One may replace it with a rectangular column of equivalent width w. This yields ([1], p. 514)

$$w = \frac{d}{1.18} < d \tag{4. 1}$$

From Eq. (4.1) one can find that $w \approx 1.7$ mm for the present antenna. Approximation (4.1) works better for lower frequencies.

3. Another possible approximation of the monopole in the surface code is a metal strip whose width is four times the cylinder radius – see [1], p. 514. We will use this approximation since it requires a smaller number of unknowns. In either case, a *fine* surface mesh along the monopole is necessary. This is a disadvantage of the surface patch code compared to the wire code.
4. The ground plane is modeled as a metal sheet of infinitesimal thickness.
5. The feed is modeled as a voltage delta-gap for every mesh edge between the monopole and the ground plane. The number of such edges can be arbitrary, depending on the cross-section shape of the monopole column.
6. The metal is an ideal conductor; metal losses are ignored.

b. Code

For the corresponding MATLAB code please refer to http://ece.wpi.edu/mom/ and download `example11.zip`. The equivalent Ansoft HFSS V. 9.1 project is saved in the file `example11a.zip`. The code should replicate Figs. 1-6 of this Chapter. In order to check the code functionality one may perform the operations listed in Table 1 either in full or partially.

Table 1. Summary of operations to create and model a monopole antenna.

Operation	Commands
Mesh generation **`1_mesh`** Selecting via/feed: 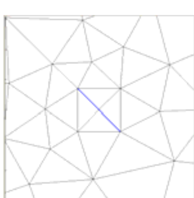	1. Run `struct2d.m` and press the `View mesh` button to see the planar mesh. Zoom in the feed area of the planar mesh to inspect the mesh structure close to the feed. Identify the role of each planar object (two rectangles and one circle) given in the GUI. - Press the `Accept mesh` button to erase the existing 3D mesh. 2. Run `struct3d.m` and do the following: - Press `OK` on the first (layer) GUI

	- Remove all **tetrahedra** from the mesh (`Select all + DONE`) - Select all **metal faces of the ground plane** (`Select all + DONE`) - When selecting **via metal patches** zoom in the feed area first. The feed edges are the two bottom edges of the metal strip. Select these two edges, one by one, by drawing a small polygon around each edge and using the `Close Polygon` button. Press `DONE.` - When selecting **feed edges** zoom in the feed area first and then repeat the above operation (selecting the via) exactly. The feed edges are the bottom edges of the metal strip. In this case they coincide with the via edges. - When selecting **top metal patches** press `DONE.` Press `OK` on the `Remove` screen. - Inspect the mesh and the feeding triangles visually. They should have a color different from that of the other metal triangles. Also, plus and minus feeding triangles have distinct colors.
BF generation **`2_basis`**	Run `wrapper.m` and inspect the resulting number of unknowns (metal edges).
MoM solution **`3_mom`**	1. Open `impedance.m`. The frequency range and the number of discrete points are given in this file. Run `impedance.m`. 2. Run `comp_s.m` to inspect the return loss and impedance bandwidth. 3. Run `radpattern.m` to obtain the patterns (cross-/co-pol) in the E-plane (elevation plane). 4. Run `nearfield.m` to inspect the charge/current distribution of the antenna.

c. Mesh

Fig. 4.2 shows the monopole antenna mesh obtained after the mesh generation operation. The final surface/volume mesh is inspected with the script `struct3d.m`. Special attention should be paid to feed assembly (selecting the via patches for the feed column, and identifying the feeding edges with `struct3d.m`). The visual feed inspection is also done with `struct3d.m.`

There is a difference in the feed assembly between the MoM voltage gap and the corresponding Ansoft dipole project shown in Fig. 4.2c. The lumped port in Ansoft is defined on a finite-width circular ring face between the monopole and the rest of the ground plane.

When the outer radius of this face tends to its inner radius, both definitions of the lumped port should coincide with each other.

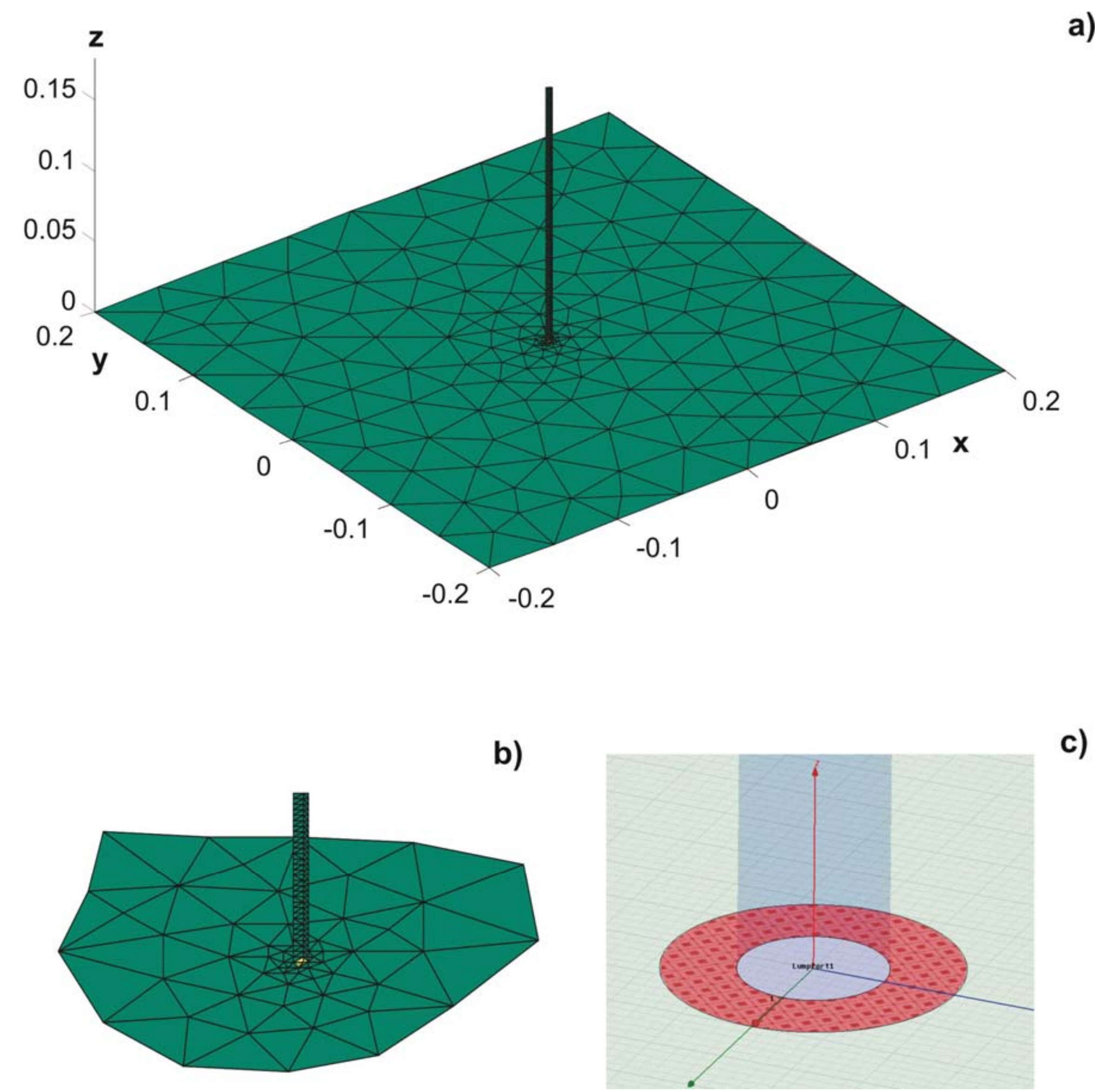

Fig. 4.2. a) – Metal mesh created by `struct3d.m`; b) – voltage gap feed implemented in MATLAB for bottom feeding edges; c) – Ansoft lumped port with the port face (a ring) between the ground plane (a hole was cut in the ground plane) and the monopole. The voltage is given along a feed line in this face.

d. Input impedance

The antenna input impedance $Z_A = R_{in} + jX_{in}$ is calculated in the script `impedance.m` at the discrete frequency steps. The number of steps and the frequency range are specified in that script. The simplest voltage gap feed model is given in the script; it can be replaced by an extended gap model [4] or the magnetic frill model [1]. The present antenna mesh has 1229 metal unknowns and needs about 1 second per frequency step on a PIV 3.6 GHz.

The antenna resonance occurs when the reactance X_{in} becomes zero at a certain frequency. The resonant frequency by inspection is close to 400 MHz The script `impedance.m` simultaneously computes the power, $P_{\text{feed}} = P_{in}$, delivered to the antenna in the feed at every frequency, i.e.

$$P_{\text{in}} = \frac{1}{2}\text{Re}(IV^*) \tag{4.2}$$

where I is the total current in the feed and V is the applied feed voltage (1V).

The return loss (magnitude of the antenna reflection coefficient vs. 50 Ω) in dB and the VSWR (voltage standing wave ratio, see [1])

$$\left|\Gamma\right|_{\text{dB}} = -20\log_{10}\left(\left|\frac{Z_A - 50}{Z_A + 50}\right|\right) \tag{4.3a}$$

$$\text{VSWR} = \frac{1+\left|\Gamma\right|}{1-\left|\Gamma\right|} \tag{4.3b}$$

is calculated in the script `impedance.m`. Note that the MATLAB figure shows the negative values for the return loss. The antenna center frequency is the frequency at which the return loss attains its maximum value. This value is close to 400 MHz, although the antenna is not matched to 50 Ω. Fig. 4.3 shows the output of the scripts `comp_z.m` and `comp_s.m` for the impedance and return loss. These scripts compare the MoM solution with the Ansoft HFSS solution. Whilst there is a good agreement at low frequencies, the impedance curves show a significant error for the higher frequencies, when the monopole length is the half wavelength in free space. Generally, the surface patch code is not very appropriate for the modeling of thin-wire antennas.

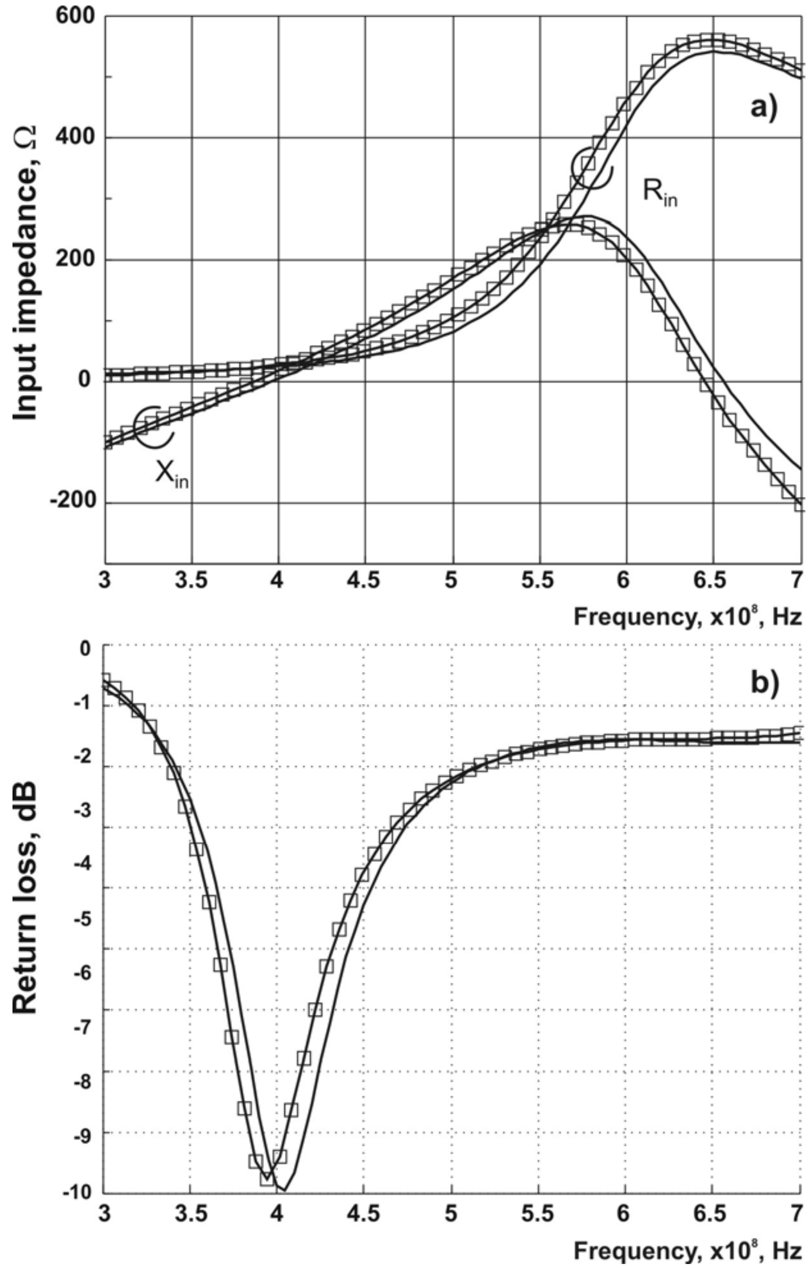

Fig. 4.3. Return loss for the monopole antenna shown in Fig. 4.1. Squared curves – MoM solution. Solid curves – Ansoft HFSS solutions.

e. Radiation pattern – total directivity/gain

The radiation characteristics are calculated in the script `radpattern.m.` The script accepts a frequency value, searches for the closest MoM solution saved in the file `out.mat` (output of `impedance.m`) and then calculates the electric and magnetic fields based on this solution – see section 7.3 of Chapter VII. The fields are first calculated over a large sphere of radius *R* in order to find the total radiated power, P_{rad}

$$P_{\mathrm{rad}} = \int_S \vec{W} \cdot \vec{n} ds, \quad \vec{W} = \frac{1}{2}\mathrm{Re}\left[\vec{E} \times \vec{H}^*\right] \tag{4.4}$$

Herein $\vec{W}$ is the time-averaged Poynting vector, and $\vec{n}$ is the outer normal to the sphere surface. This value is compared to the already found antenna feed power, P_{in}. The ratio of these two powers characterizes the antenna radiation efficiency e_{cd},

$$e_{cd} = \frac{P_{\mathrm{rad}}}{P_{\mathrm{in}}} \tag{4.5}$$

The relative difference between these two powers characterizes the antenna losses. Since a lossless dielectric and a perfect metal conductor have been used, the relative difference is expected to be small. The script `radpattern.m` gives a relative difference of 0.36% in the present case.

Next, the total or absolute logarithmic directivity, *D*, on the sphere surface is found in the form

$$D(\vec{r}) = 10\log_{10}\left(\frac{4\pi R^2 \vec{W}(\vec{r}) \cdot \vec{n}(\vec{r})}{P_{\mathrm{rad}}}\right), \quad |\vec{r}| = R \tag{4.6}$$

For the antenna gain, *G*, the total radiated power P_{rad} in Eq. (4.4) should be replaced by P_{in}. For the lossless antenna, $G = D$. The directivity plot over the sphere surface (script `radpattern.m`) for the present antenna is shown at the resonance in Fig. 4.4. One can see that the monopole pattern becomes directional due to the ground plane; however, this effect is small.

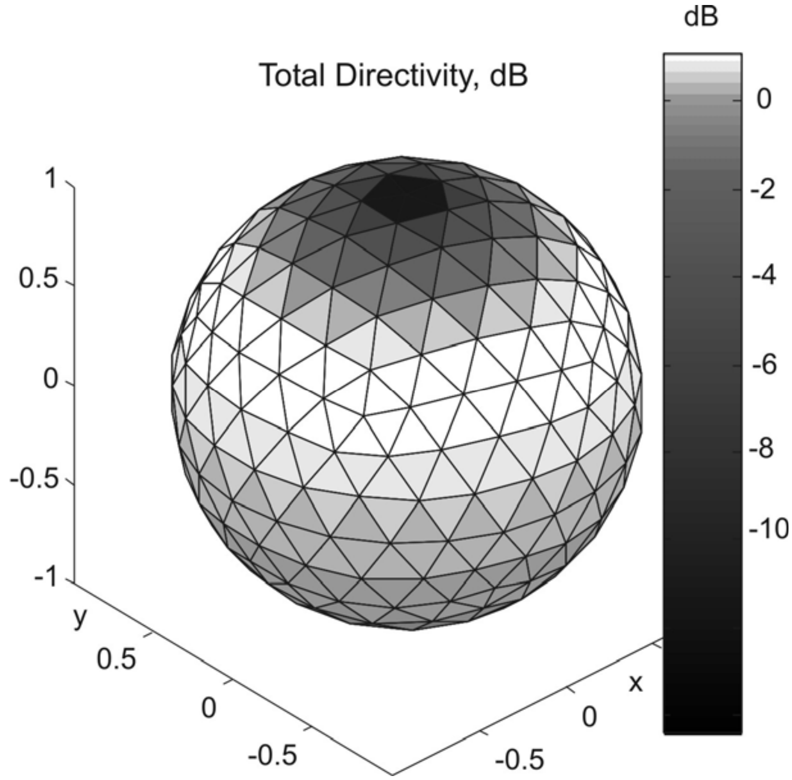

Fig. 4.4. Total directivity for the monopole antenna in Fig. 4.1 at the resonance. The maximum directivity (maximum gain in this lossless case) is approximately 1.15 dB.

f. Radiation pattern – co-polar and cross-polar components

For the elevation radiation patterns, one uses the elevation angle $\theta \in 0, \pi$ as an independent variable in the script `radpattern.m`. Then, the *xz*- and *yz*-planes are described by

$$\phi = 0 \quad \text{for the } xz\text{-plane}$$
$$\phi = \frac{\pi}{2} \quad \text{for the } yz\text{-plane} \tag{4.7}$$

in spherical coordinates. Instead of the Cartesian components of the electric field, one needs its spherical components found in the script `radpattern.m`

$$E_\theta = E_x \cos\theta \cos\phi + E_y \cos\theta \sin\phi - E_z \sin\theta \tag{4.8}$$

$$E_{\phi} = -E_x \sin\phi + E_y \cos\phi \tag{4.9}$$

Then, the co-polar directivity (directivity of the in-plane electric field component) or simply the co-polarization yields

$$D(\vec{r}) = 10\log_{10}\left(\frac{4\pi R^2 W}{P_{\mathrm{rad}}}\right), \quad W = \frac{1}{2\eta}\left|E_{\theta}\right|^2 \tag{4.10}$$

for any fixed large radius *R*. Similarly, the cross-polar directivity (directivity of the out-of-plane electric field component) or the cross-polarization gives

$$D(\vec{r}) = 10\log_{10}\left(\frac{4\pi R^2 W}{P_{\mathrm{rad}}}\right), \quad W = \frac{1}{2\eta}\left|E_{\phi}\right|^2 \tag{4.11}$$

Eqs. (4.10), (4.11) are only valid for the elevation radiation patterns.

The script `radpattern.m` outputs two radiation patterns for the present antenna, in the *E*-plane (the *yz*-plane in our case). In this plane, the co-polar directivity clearly dominates. The offset for the MATLAB polar plot is given as 60 dB. The output of this script is shown in Fig. 4.5 (the offset is removed).

g. Near fields

It is also desired to inspect the near field distributions in the antenna volume or on the antenna surface. The script `nearfield.m` finds and displays such distributions at a given frequency. The script accepts a frequency value, searches for the closest MoM solution saved in the file `out.mat` (output of `impedance.m`) and then calculates the electric and magnetic near fields based on this solution – see section 7.3 of Chapter VII. The electric current density on the metal surface and the associated free charge distribution are found using the MoM solution for the metal patches. Fig. 4.6 shows the typical current distribution for the monopole antenna.

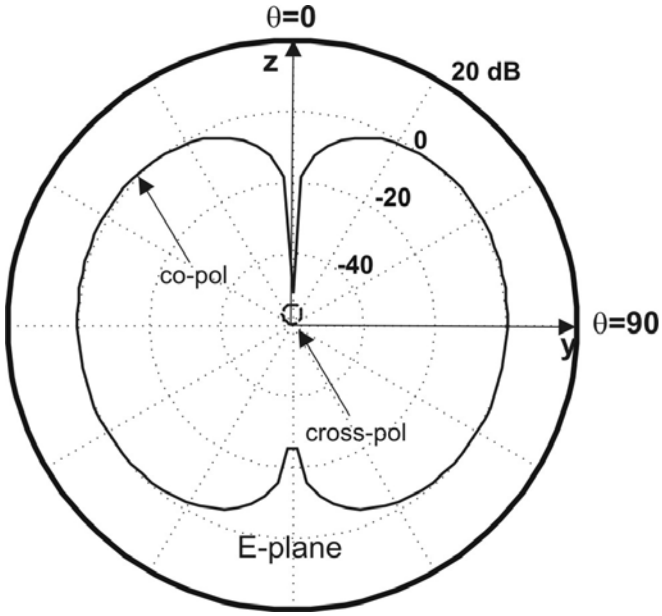

Fig. 4.5. Directivity of the co-polar and cross-polar fields vs. elevation angle for the monopole antenna at the resonant frequency, in the *E*-plane.

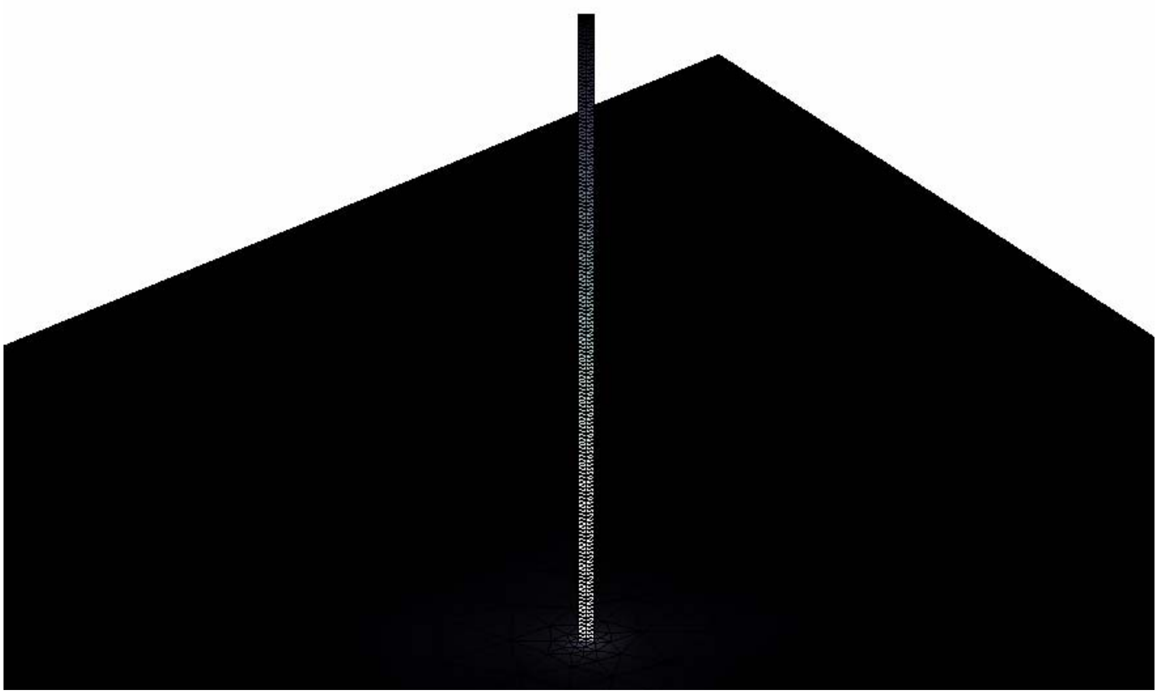

Fig. 4.6. Typical current distribution along the lower half of the monopole antenna at the resonant frequency. Lighter colors correspond to larger current magnitudes.

4.2 Loaded monopole

Loading of electrically small monopole antennas to improve their impedance characteristics (provide impedance matching at a smaller size, that is, height) has been employed for many decades. Such techniques may include end-disks or top hats [5], dielectric coatings [6], or both techniques combined [7, 8]. The antenna size can be reduced significantly, but at the expense of decreasing the impedance bandwidth. In this section we consider a top hat dielectric-loaded monopole.

a. Geometry

This example is adopted from Ref. 8 (Fig. 4.6) and describes a top-hat dielectric-loaded monopole with $\varepsilon_r = 10.0$. The antenna geometry is shown in Fig. 4.7. Here, $\varepsilon_r = 10.0$ for dielectric #1. Dielectric #2 is air.

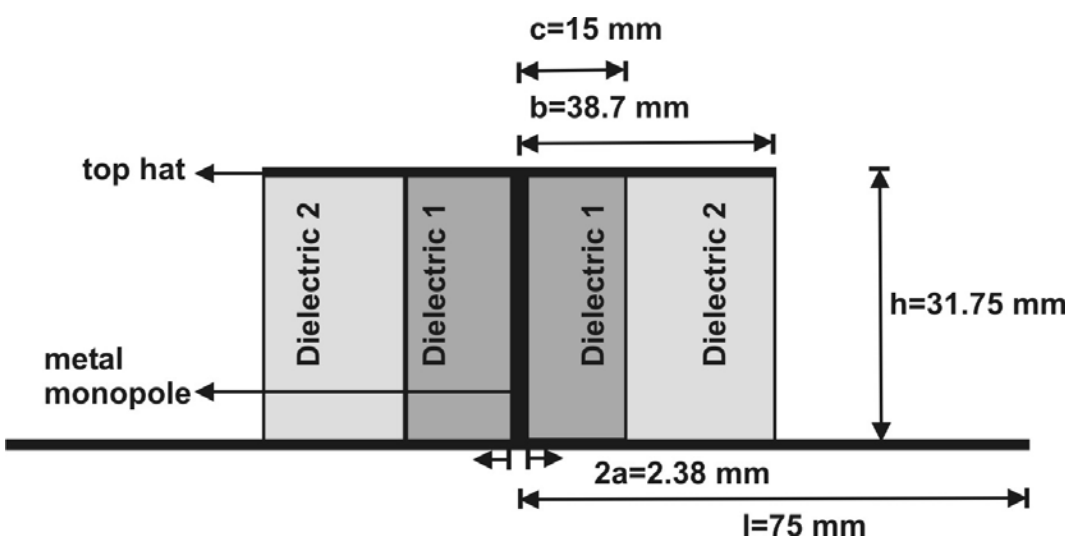

Fig. 4.7. Top hat dielectric-loaded monopole [8].

The antenna has the following features:

1. Both the top hat and the dielectric reduce the physical size of the monopole antenna (decrease its resonant frequency) but at the expense of reducing the bandwidth. The dielectric loading plays a major role in reducing the bandwidth.
2. Although the dielectric loading is relatively thick, no dielectric resonant (DR) modes are excited yet.

b. Code

For the corresponding MATLAB code please refer to http://ece.wpi.edu/mom/ and download `example42.zip`. The equivalent Ansoft HFSS V. 9.1 project is saved in the file `example42a.zip`. The code should replicate Figs. 7-11 of this Chapter. In order to check the code functionality one may follow operations listed in Table 1 at the beginning of this Chapter above either in full or partially. The creation of this structure is essentially identical to the monopole antenna considered in Section 4.1, including the antenna feed. The dielectric tetrahedra must be removed from:

a. the feed column
b. the entire antenna volume except for the coating cylinder.

Fig. 4.8 shows the dielectric mesh obtained after running the script `struct3d.m`. The circular feed column is replaced by a rectangular column according to Eq. (4.1).

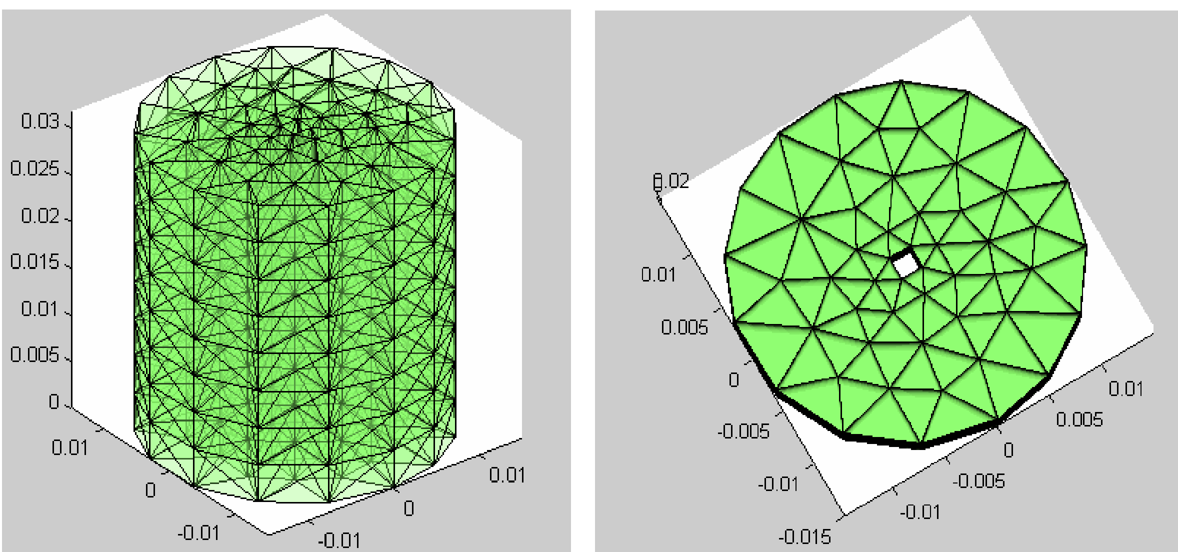

Fig. 4.8. Tetrahedral mesh obtained after running the script `struct3d.m`.

c. Mesh

Fig. 4.9 shows the complete antenna mesh obtained after the mesh generation operation. The final surface/volume mesh is inspected with the script `struct3d.m`.

Special attention should be paid to feed assembly (removing tetrahedra from the feed, selecting the via patches for the feed column, and identifying the feeding edges with `feed.m`). The visual feed inspection is also done with `struct3d.m`. Running the script `feed.m` should give eight feeding edges – two for each side of the metal column.

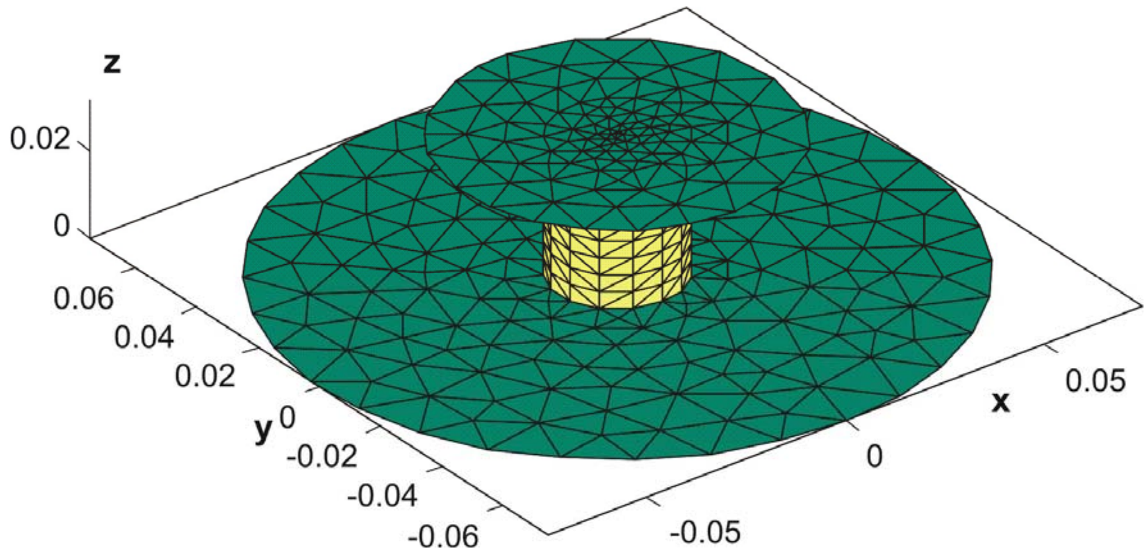

Fig. 4.9. a) – Metal-dielectric mesh for the patch antenna created by `struct3d.m`. The feed column is not seen. The lighter color corresponds to dielectric faces.

d. Input impedance

The antenna input impedance $Z_A = R_{in} + jX_{in}$ is calculated in the script `impedance.m` at discrete frequency steps. The number of steps and the frequency range are specified in that script. The present antenna has a mesh with 3296 unknowns (986 metal unknowns and 2310 dielectric unknowns) and needs about 15.3 seconds per frequency step on a PIV 3.6 GHz. The total time for 50 frequency steps is thus 15 minutes. Fig. 4.10 shows the output of the script `impedance.m` compared to the equivalent Ansoft HFSS solution (a circular column feed with r=1.19 mm is used) obtained using a mesh with 39,000 tetrahedra, a PML enclosure, and an interpolating frequency sweep. This result is obtained by running the script `comp_z.m`. The Ansoft solution shown in Fig. 4.10 requires about 40 minutes of CPU time on the same machine.

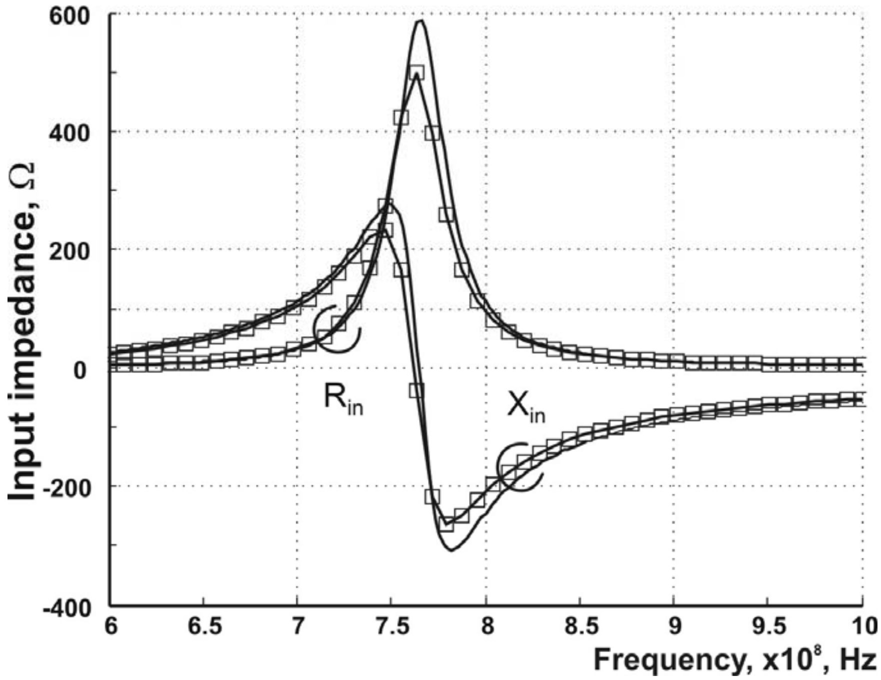

Fig. 4.10. Input impedance curves for the loaded monopole antenna shown in Fig. 4.8. Squared curves – MoM solution for the resistance/reactance; solid curves – Ansoft HFSS solution.

The antenna resonance occurs when the reactance X_{in} becomes zero at a certain frequency. The resonant frequency is close to 760 MHz in Fig. 4.10. Note that both the MoM solution and the Ansoft HFSS solution could be run at a smaller number of unknowns. For the MoM solution, for example, one can reduce the number of layers in the dielectric column. However, a larger error in the resonant frequency will be observed in both cases.

The resonant frequency reported in [8] is somewhat larger, about 800 MHz (see Fig. 4.6 of Ref. [8]); however, the impedance shape remains the same. The shift in the resonant frequency may be explained by the finite, relatively small ground plane used here (the solution in [8] assumes an infinite ground plane).

The return loss (magnitude of the antenna reflection coefficient vs. 50 Ω) is calculated in the script `comp_s.m`. Note that the MATLAB figure shows the negative values for the return loss. This antenna is not matched to 50 Ω, so its impedance bandwidth is not considered here.

e. Radiation pattern – total directivity/gain

The radiation characteristics are calculated in the script `radpattern.m` – see section 4.1 for a description of that script. The script accepts a frequency value, searches for the closest MoM solution saved in the file `out.mat` (output of `impedance.m`) and then calculates the electric and magnetic fields based on this solution – see section 7.3 of Chapter VII. The radiation patterns of the loaded monopole are very similar to those of the unloaded monopole and are not shown here.

The script `radpattern.m` gives a relative difference of 0.7% between the radiated and the feed power in the present case at 0.76 GHz.

f. Near fields

It is desired to inspect the near field distributions in the antenna volume or on the antenna surface. The script `nearfield.m` finds and displays such distributions at a given frequency. The script accepts a frequency value, searches for the closest MoM solution saved in the file `out.mat` (output of `impedance.m`) and then calculates the electric and magnetic near fields based on this solution – see section 7.3 of Chapter VII. The fields are calculated at the center of every tetrahedron in the dielectric mesh. The bound surface charge density on the dielectric surface is found using the MoM solution. Next, the electric current density on the metal surface and the associated free charge distribution are found using the MoM solution for the metal patches. In the case of the loaded monopole, the DR modes are not developed and the inspection of the dielectric fields does not add much significance to the analysis (the fields are mostly concentrated around the feed). It is interesting to inspect the current distribution on the metal surface – see Fig. 4.11. In particular, one can observe a large current on the top of the monopole, thus giving rise to a significant magnetic field in that region. This large current indicates that the top hat significantly contributes to the effective length of the antenna.

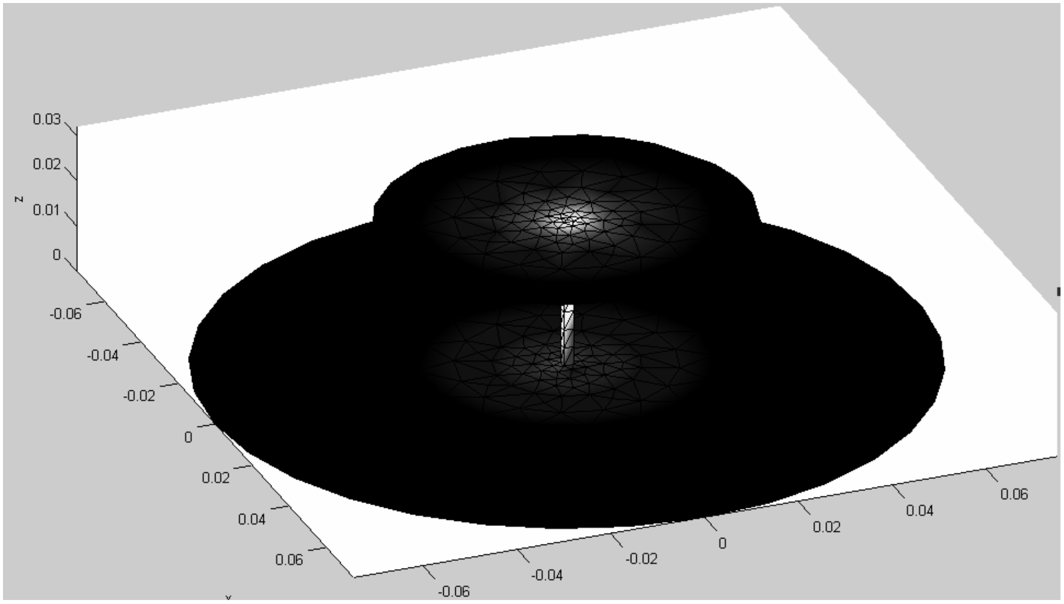

Fig. 4.11. Surface current distribution on the metal surface. Lighter colors correspond to larger current magnitudes.

4.3 Baseline planar-inverted F-antenna (PIFA)

It is well known that the monopole is the counterpart of a half-wave dipole that is obtained using the metal ground plane in the electrical symmetry plane (with the tangential *E*-field equal to zero). Similarly, the PIFA (the quarter-wave microstrip antenna) is the counterpart of the half-wave patch (see Chapter II) obtained using the metal ground plane in the symmetry plane of the TM patch antenna cavity mode (in the middle of the half-wave patch). Here, the electric field tangential to the ground plane also becomes zero. The PIFA cavity is normally rectangular (approximately half-square).

The PIFA, originally introduced in [9, 10], is one of the most popular antenna designs for wireless communications [11-14]. PIFA's inherent bandwidth is higher than the bandwidth of the conventional patch antenna (since a thick air substrate is used). Furthermore, it can be considerably enhanced.

a. Geometry

This example is adopted from Refs. [9, 11] and describes the original PIFA at 1.5 GHz. The antenna geometry is shown in Fig. 4.12. Here, $\varepsilon_r = 1$ (no dielectric substrate is used). The feed does not have to be on the edge and can be moved vertically toward the patch centerline [14] keeping the distance from the shorting ground plane the same.

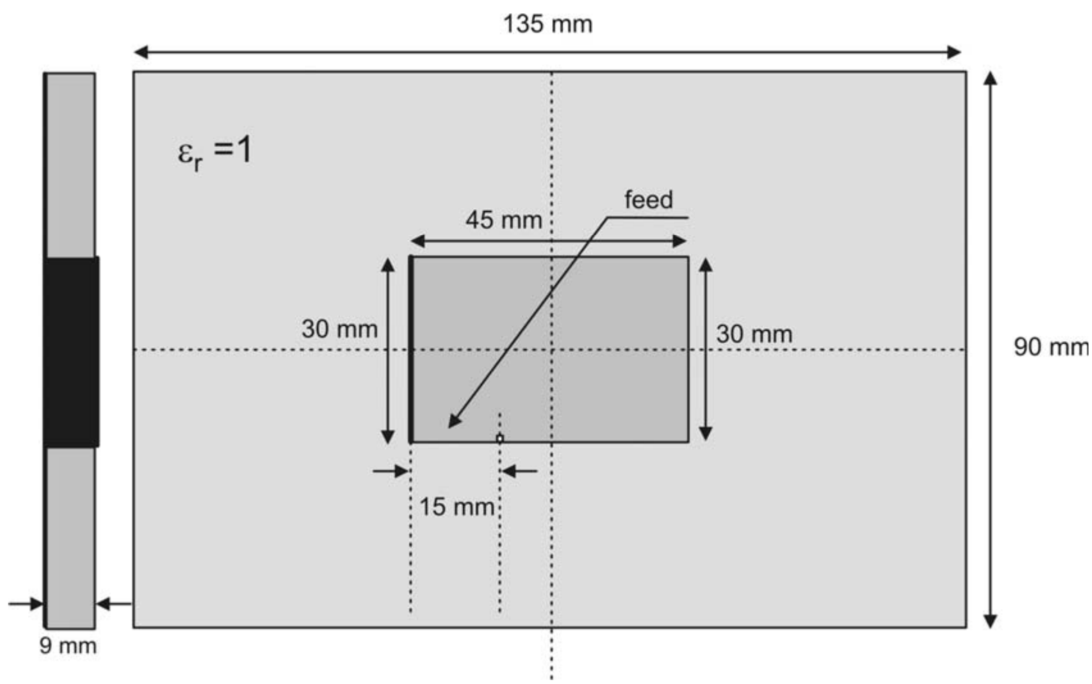

Fig. 4.12. PIFA geometry (top and side view).

The antenna has the following features:

1. The ground plane is finite. This is in contrast to Refs. [9, 11].
2. Since no exact feed diameter was reported, the rectangular feed column is chosen to be 0.5 mm in width. The width variation in the range 0.5-1.5 mm does not significantly alter the results.

b. Code

For the corresponding MATLAB code please refer to http://ece.wpi.edu/mom/ and download `example43.zip`. The equivalent Ansoft HFSS V. 9.1 project is saved in the file `example43a.zip`. The code should replicate Figs. 12-17 of this Chapter. In order to check the code functionality one may perform the operations listed in Table 1 at the beginning of this Chapter either in full or partially. The creation of this structure is essentially identical to the monopole antenna considered in Section 4.1, including the antenna feed. The dielectric tetrahedra must be removed from the entire volume. The shorting ground plane should be identified at the via stage in the script `struct3d.m`. The top patch should be selected using the polygon tool – `close polygon`. It is recommended to zoom in on the mesh and make sure that all the triangles are selected properly for the top patch. If this is not the case, they need to be selected or deselected individually.

c. Mesh

Fig. 4.13 shows the metal mesh obtained after running the script `struct3d.m`.

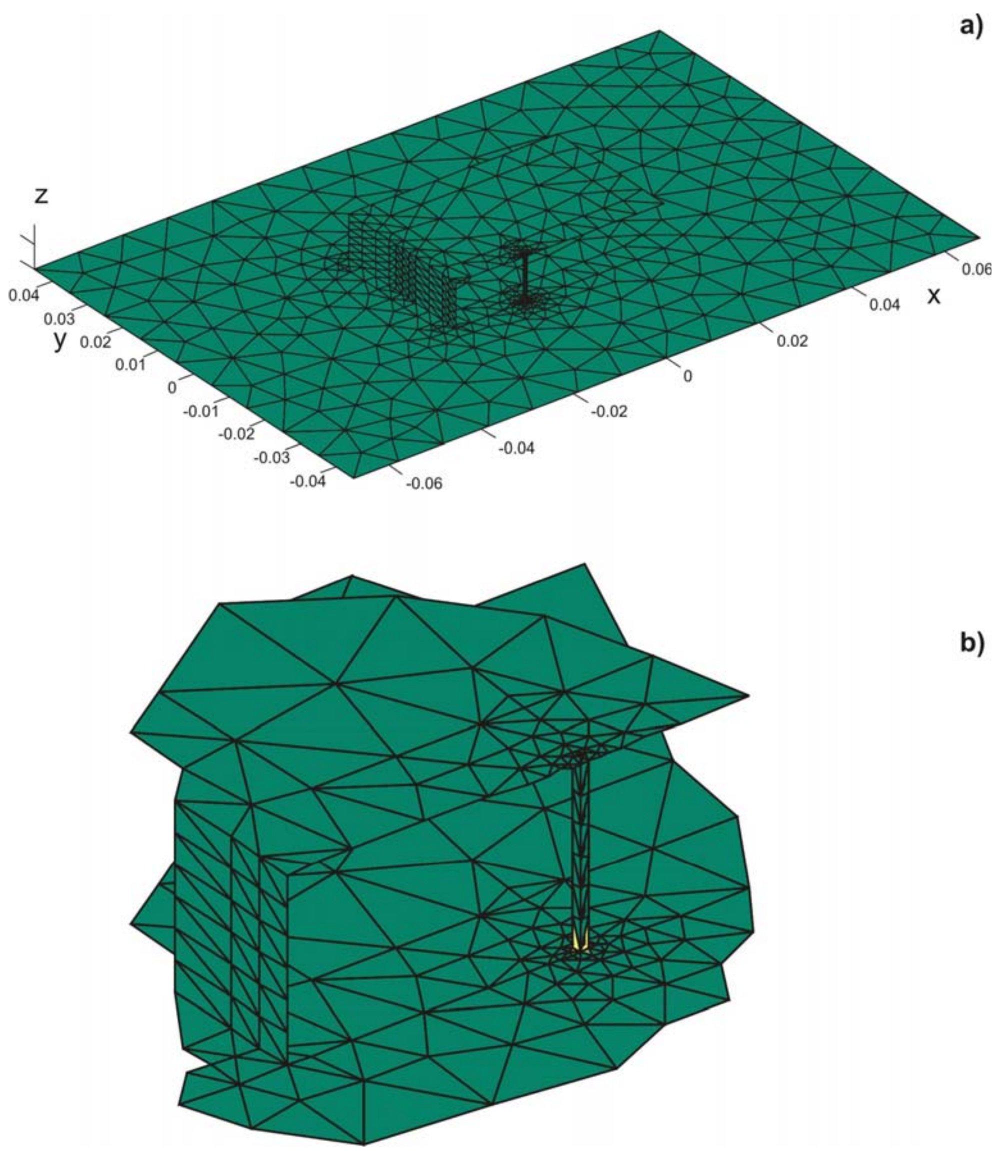

Fig. 4.13. Complete metal mesh obtained after running the script `struct3d.m`. The feed triangles/edges are seen (enlarged in Fig. 4.13b).

Special attention should be paid to the via and feed assembly. Loading the data file `struct3d.mat` should give eight feeding edges in the array `FeedIndexes` – two for each side of the metal column.

d. Input impedance

The antenna input impedance $Z_A = R_{in} + jX_{in}$ is calculated in the script `impedance.m` at the discrete frequency steps. The number of steps and the frequency range are specified in that script. The present antenna mesh has 1519 unknowns and needs about 1 second per frequency step on a PIV 3.6 GHz. The total time for 60 frequency steps is thus about 1 minute. Fig. 4.14a shows the output of the script `impedance.m` compared to the equivalent Ansoft HFSS solution (a rectangular column feed is used) obtained using a mesh with about 20,000 tetrahedra, a radiating enclosure, and an interpolating frequency sweep. This result is obtained by running the script `comp_z.m`. The Ansoft solution shown in Fig. 4.14 takes about 20 minutes on the same machine. The antenna resonance occurs when the reactance X_{in} becomes zero at a certain frequency. The resonant frequency is close to 1.35 GHz in Fig. 4.14.

The return loss (magnitude of the antenna reflection coefficient vs. 50 Ω) is calculated in the script `comp_s.m`. – Fig. 4.14b. Note that the MATLAB figure shows the negative values for the return loss. This antenna is now matched to 50 Ω at 1.5 GHz, which is a rather significant difference from the physical resonance. Also note that Fig. 4.14b is in very close agreement with the corresponding FDTD simulation results for the PIFA given in Ref. [11], pp. 202-203.

Both the MoM solution and the Ansoft solution could be run at a smaller number of unknowns. For the MoM solution, for example, one can reduce the mesh quality. For the Ansoft solution, one can use 3 to 5 passes. However, a larger error in the return loss behavior – impedance bandwidth – will be observed in both cases.

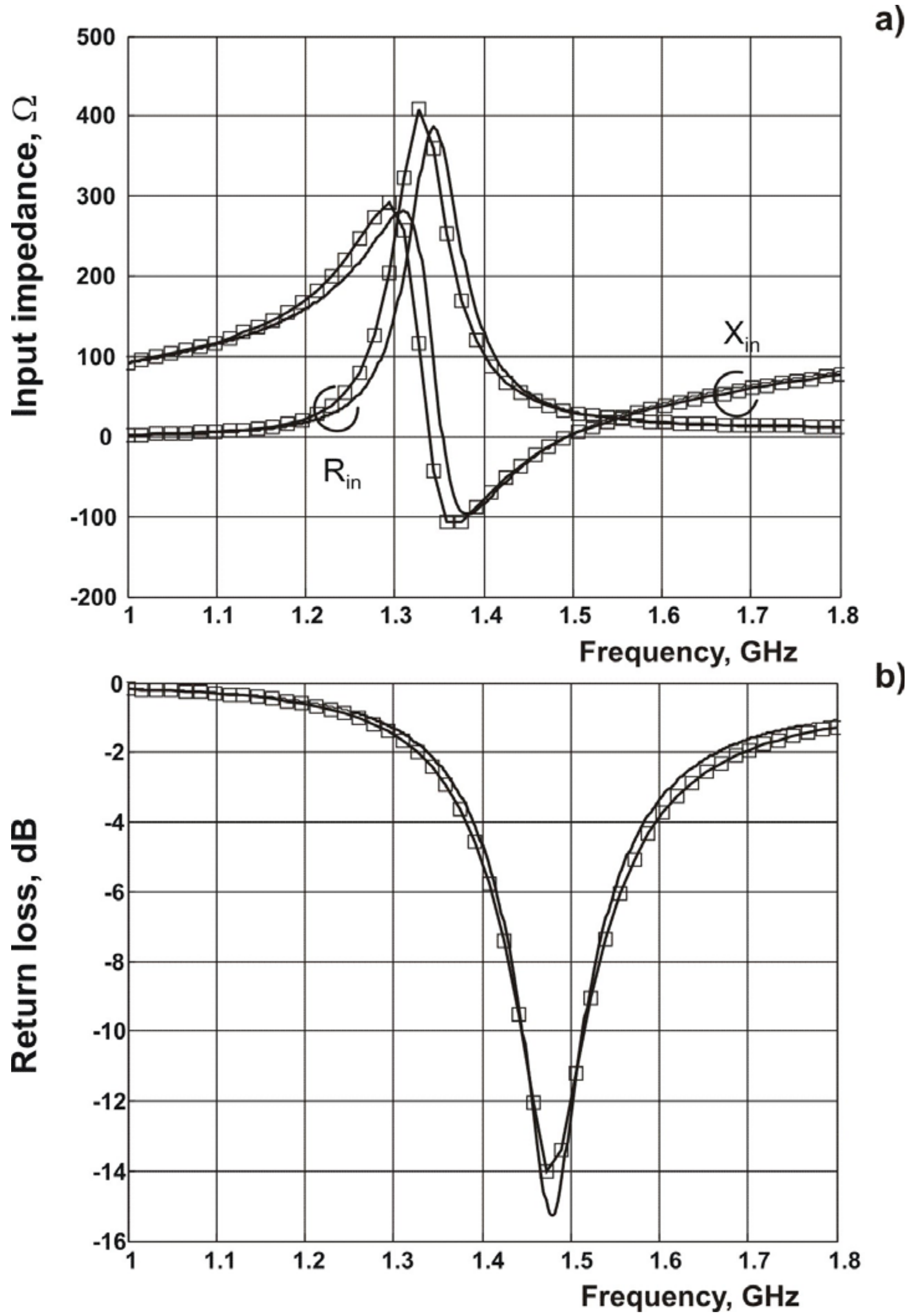

Fig. 4.14. a) - Input impedance curves; b) – return loss curves for the PIFA antenna shown in Fig. 4.12. Squared curves – MoM solution for the resistance/reactance; solid curves – Ansoft HFSS solution.

e. Radiation pattern – total directivity/gain

The radiation characteristics are calculated in the script `radpattern.m` – see section 4.1 for a description of that script. The script accepts a frequency value, searches for the closest MoM solution saved in the file `out.mat` (output of `impedance.m`) and then calculates the electric and magnetic fields based on this solution – see section 7.3 of Chapter VII.

The directivity plot over the sphere surface (script `radpattern.m`) for the present antenna is shown at 1.5 GHz (center of the impedance bandwidth) in Fig. 4.15. One can see that the symmetric radiation pattern is slightly distorted. The script `radpattern.m` gives a relative difference of 0.56% between the radiated and the feed power in the present case.

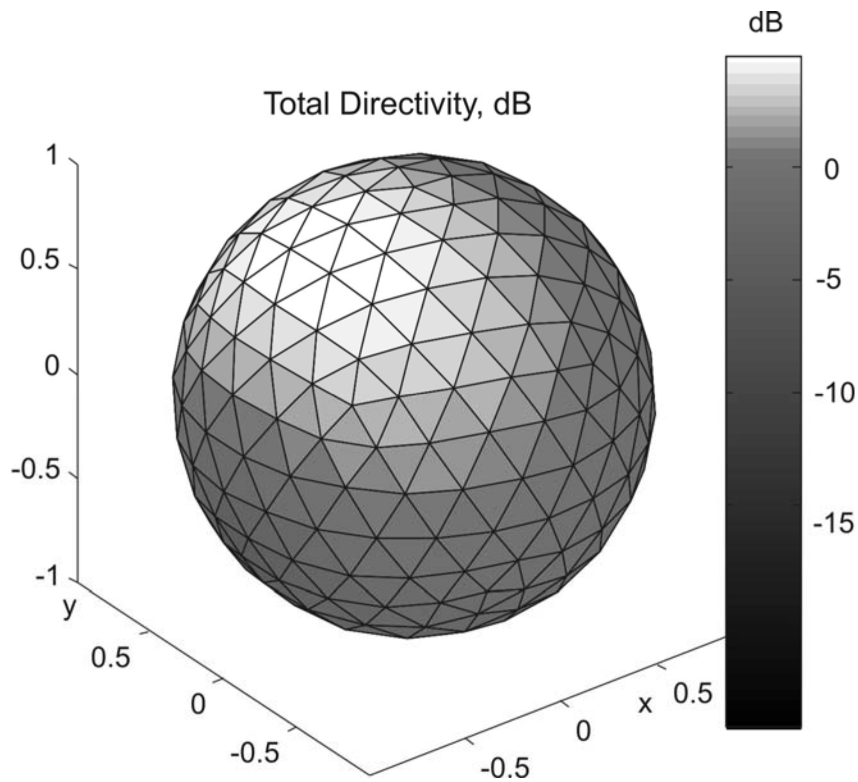

Fig. 4.15. Total directivity for the PIFA antenna in Fig. 4.12 at 1.5 GHz. The maximum directivity (maximum gain in this lossless case) is approximately 5 dB.

f. Radiation pattern – co-polar and cross-polar components

The co-polar and cross-polar directivity components are found in a manner similar to the approach described in Section 2.1. However, we are interested in the *E*-plane radiation patterns (the *xz*-plane) for the present configuration.

The script `radpattern.m` outputs two radiation patterns (co-pol and cross-pol components) for the present antenna, in the *E*-plane (the *xz*-plane in our case). In this plane, the co-polar directivity dominates. The offset for the MATLAB polar plot is given as 60 dB. The script `comp_r.m` (which should be run after `radpattern.m`) compares these radiation patterns with the corresponding Ansoft HFSS radiation patterns. The output of this script is shown in Fig. 4.16 (the offset is removed). One can see a reasonably good agreement.

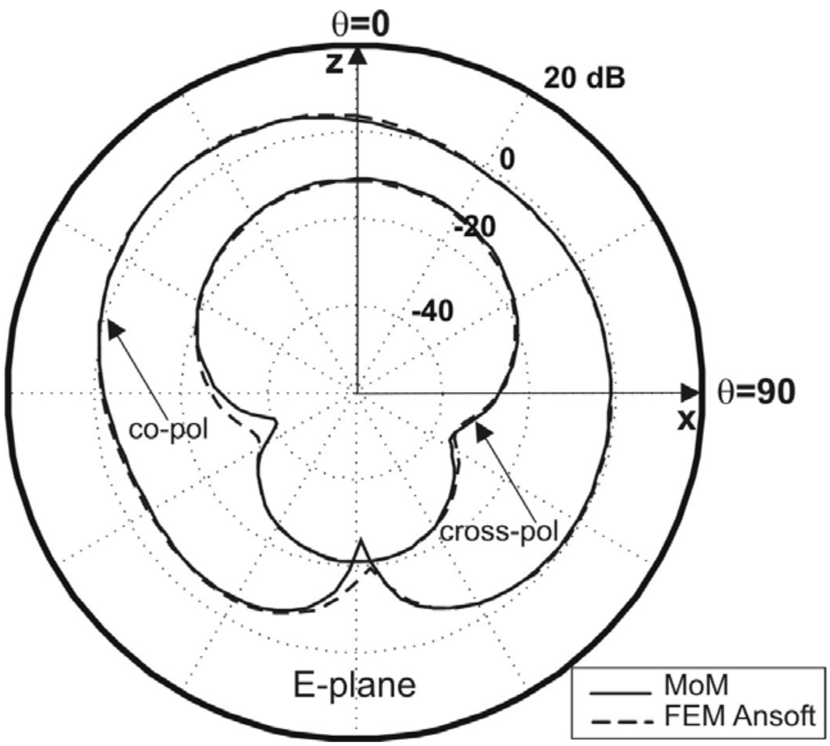

Fig. 4.16. Directivity of the co-polar and cross-polar fields vs. elevation angle for the patch antenna at the center frequency (1.5 GHz) in the *E*-plane. The MoM solution is shown by a solid curve; the Ansoft solution is given by a dashed curve.

The front-to-back ratio for the present patch antenna is small, and the antenna is rather "omnidirectional" in every plane.

g. Near fields

It is desired to inspect the near field distributions in the antenna volume or on the antenna surface. The script `nearfield.m` finds and displays such distributions at a given frequency. In the case of the PIFA the TM mode is not as prominent as for the half-wave patch (Chapter II above). It is interesting to inspect the current distribution on the metal surface – Fig. 4.17. In particular, a large current returns from the top patch through the shorting ground plane. A large current is also observed on the side of the shorting plane that is opposite to the feed.

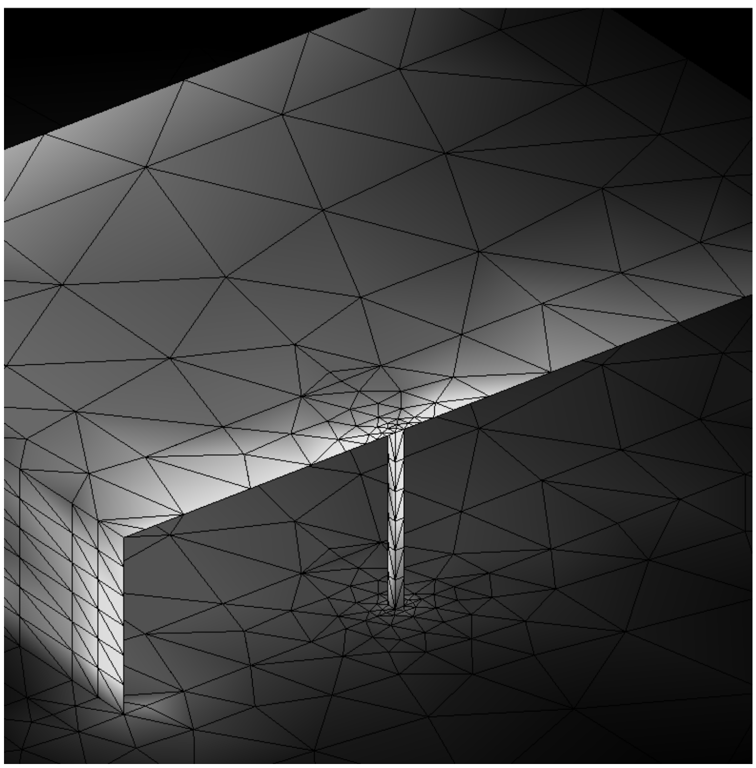

Fig. 4.17. Surface current distribution on the metal surface at 1.35 GHz. Lighter colors correspond to larger current magnitudes.

4.4 Reduced-size PIFA

This example is adopted from Refs. [9, 11] and shows how the resonant frequency of the PIFA from the previous section can be reduced by a factor of 1.5. This reduction is equivalent to a reduction in size, when the antenna is scaled to its original frequency. However, as a result, the PIFA's bandwidth decreases very significantly.

a. Geometry

The antenna geometry is shown in Fig. 4.18. Here, $\varepsilon_r = 1$ (no dielectric substrate is used).

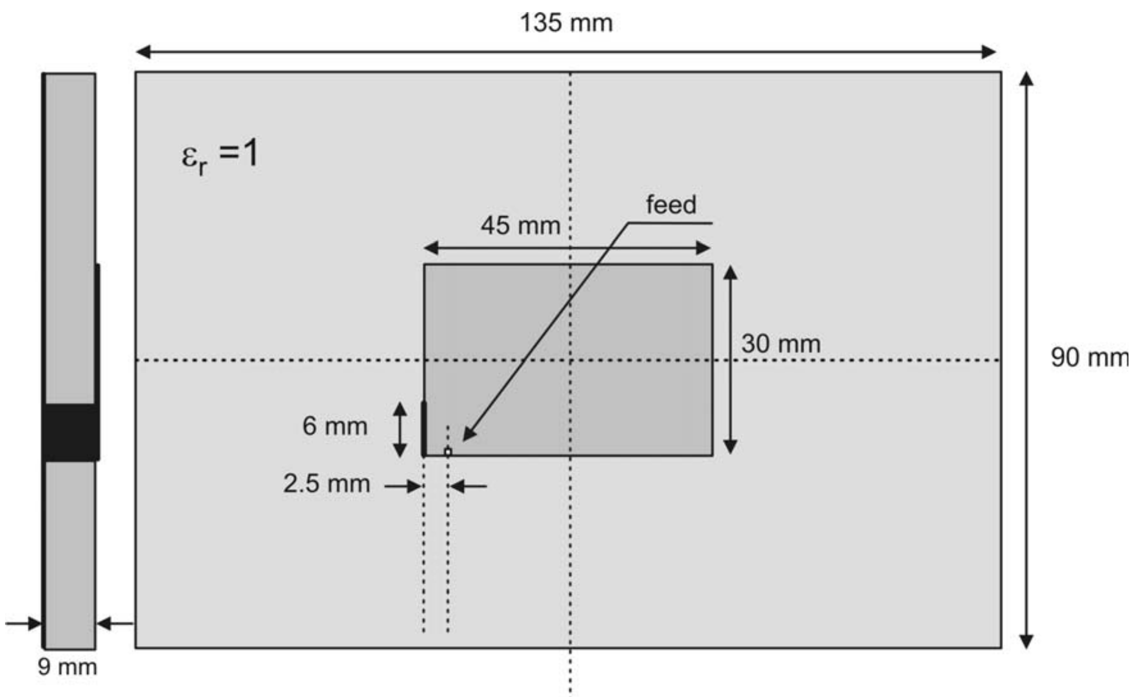

Fig. 4.18. PIFA geometry (top and side view).

The antenna has the following features:

1. The feed is in close proximity to the shorting ground plane. Therefore, the impedance behavior (impedance matching rather than resonant frequency) is very sensitive to the feed position.
2. The ground plane is finite in contrast to [9, 11]. Therefore, to achieve the proper impedance matching the feed is shifted by 0.5 mm compared to [9, 11] toward the short circuit plane.

3. Since no exact feed diameter was reported, the rectangular feed column is chosen to be 0.5 mm in width.

b. Code

For the corresponding MATLAB code please refer to http://ece.wpi.edu/mom/ and download `example44.zip`. The equivalent Ansoft HFSS V. 9.1 project is saved in the file `example44a.zip`. The code should replicate Figs. 18-23 of this Chapter. In order to check the code functionality one may perform the operations listed in Table 1 at the beginning of this Chapter either in full or partially.

c. Mesh

The creation of this structure is almost identical to the PIFA antenna considered in Section 4.3 but the shorting ground plane is truncated. Fig. 4.19 shows the metal mesh obtained after running the script `struct3d.m`.

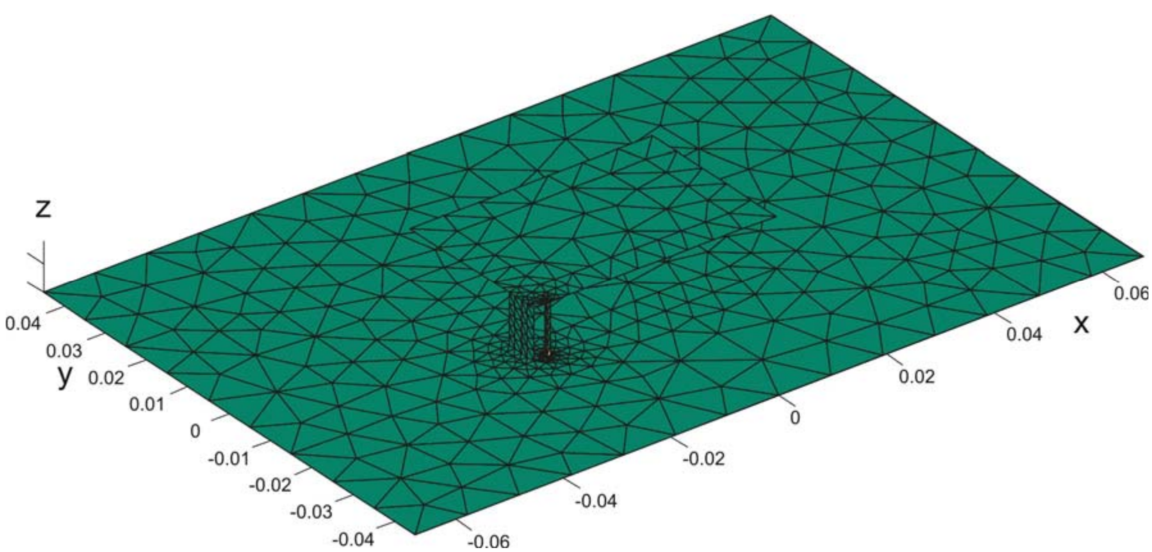

Fig. 4.19. Complete metal PIFA mesh obtained after running the script `struct3d.m`.

d. Input impedance

The antenna input impedance $Z_A = R_{in} + jX_{in}$ is calculated in the script `impedance.m` at the discrete frequency steps. The number of steps and the frequency range are specified in that script. The present antenna mesh has 1255 unknowns and needs about 0.8 second per frequency step on a PIV 3.6 GHz. Fig. 4.20a shows the output of the script `impedance.m` compared to the equivalent Ansoft HFSS solution (rectangular column feed is used) obtained using a mesh with about 20,000 tetrahedra, a radiating enclosure, and an interpolating frequency sweep.

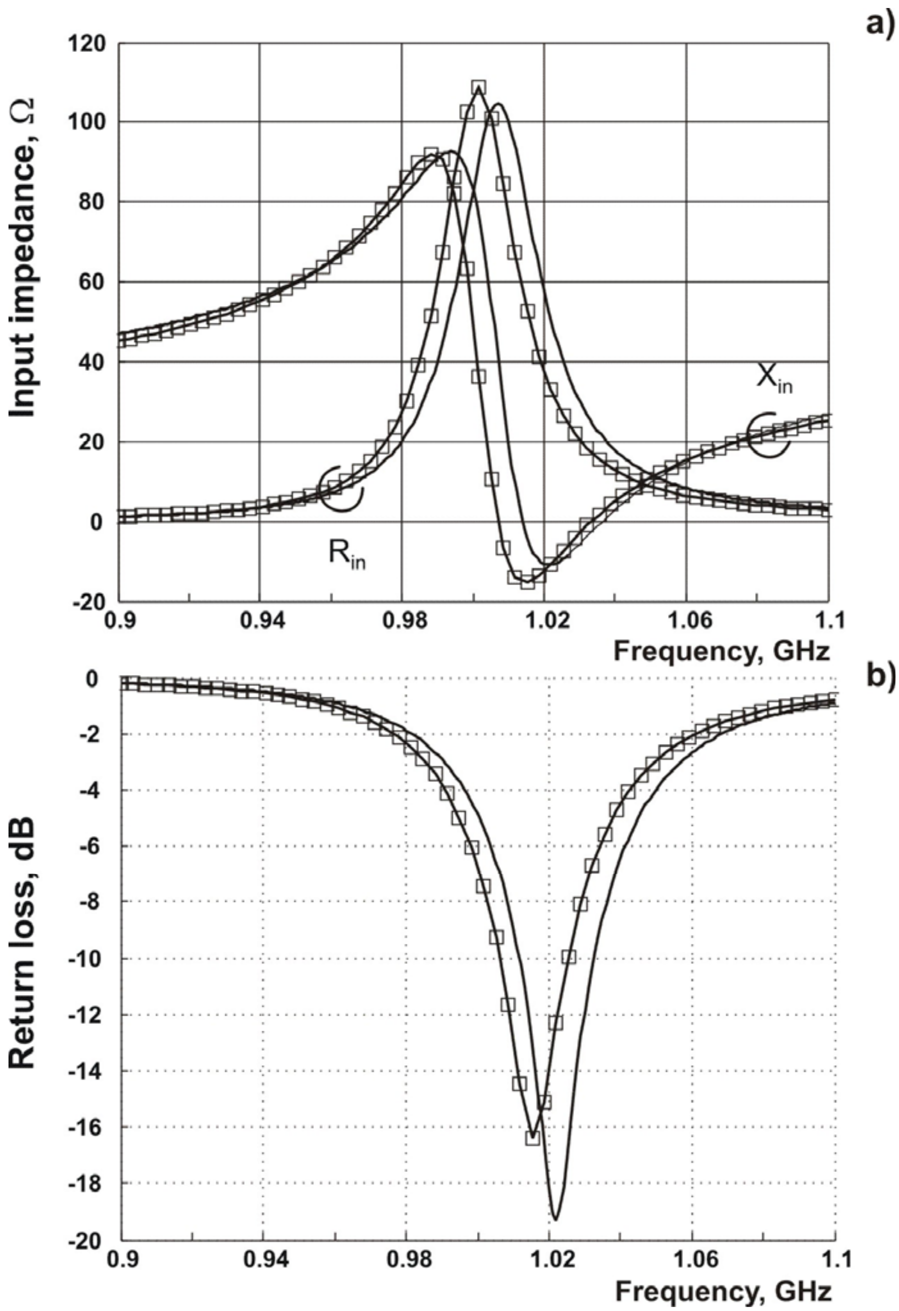

Fig. 4.20. a) - Input impedance curves; b) – return loss curves for the PIFA antenna shown in Fig. 4.18. Squared curves – MoM solution for the resistance/reactance; solid curves – Ansoft HFSS solution.

This result is obtained by running the script `comp_z.m`. The Ansoft solution shown in Fig. 4.20 takes about 20 minutes on the same machine. The antenna resonance occurs when the reactance X_{in} becomes zero at a certain frequency. The resonant frequency is close to 1.01 GHz in Fig. 4.20.

The return loss (magnitude of the antenna reflection coefficient vs. 50 Ω) is calculated in the script `comp_s.m`. – Fig. 4.20b. Note that the MATLAB figure shows the negative values for the return loss. This antenna is now matched to 50 Ω at 1.02 GHz, which is not much different from the physical resonance. Note that Fig. 4.20b is also in a close agreement with the corresponding FDTD simulation result for the PIFA antenna (Ref. [11], pp. 202-203).

Both the MoM solution and the Ansoft solution could be run at a smaller number of unknowns. For the MoM solution, for example, one can reduce the mesh quality. For the Ansoft solution, one can use 3 to 5 passes. However, a larger error in the return loss behavior – impedance bandwidth – will be observed in both cases.

e. Radiation pattern – total directivity/gain

The radiation characteristics are calculated in the script `radpattern.m` – see section 4.1 for a description of that script. The script accepts a frequency value, searches for the closest MoM solution saved in the file `out.mat` (output of `impedance.m`) and then calculates the electric and magnetic fields based on this solution – see section 7.3 of Chapter VII.

The directivity plot over the sphere surface (script `radpattern.m`) for the present antenna is shown at 1.02 GHz (center of the impedance bandwidth) in Fig. 4.21. One can see that the symmetric radiation pattern is slightly distorted. The script `radpattern.m` gives a relative difference of 0.57% between the radiated and the feed power in the present case. The directivity looks more omnidirectional than for the full-size PIFA antenna in Fig. 4.16.

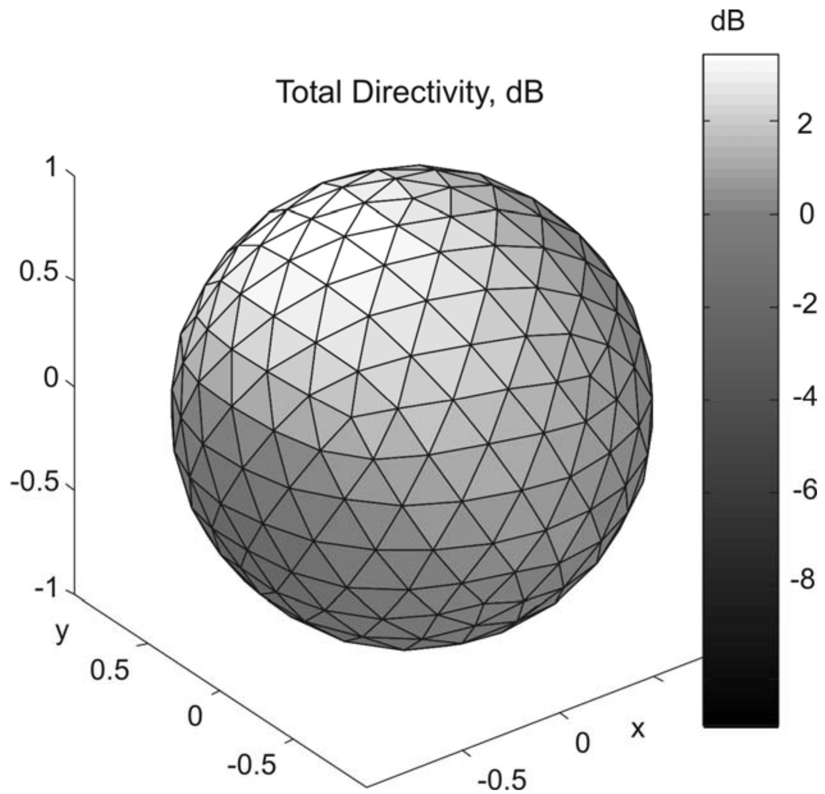

Fig. 4.21. Total directivity for the PIFA antenna in Fig. 4.18 at 1.02 GHz. The maximum directivity (maximum gain in this lossless case) is approximately 4 dB.

f. Radiation pattern – co-polar and cross-polar components

The co-polar and cross-polar directivity components are found similar to the approach described in section 2.1. However, we are interested in the *E*-plane radiation patterns (the *xz*-plane) for the present configuration.

The script `radpattern.m` outputs two radiation patterns (co-pol and cross-pol components) for the present antenna, in the *E*-plane (the *xz*-plane in our case). In this plane, the co-polar directivity dominates. The offset for the MATLAB polar plot is given as 60 dB. The script `comp_r.m` (which should be run after `radpattern.m`) compares these radiation patterns with the corresponding Ansoft HFSS radiation patterns. The output of this script is shown in Fig. 4.22 (the offset is removed). One can see a reasonably good agreement.

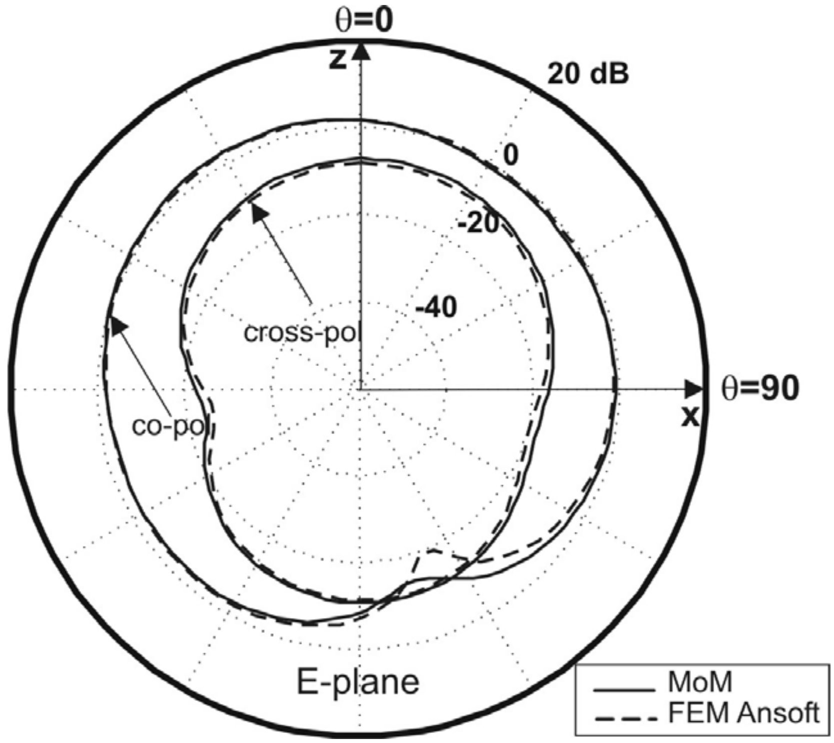

Fig. 4.22. Directivity of the co-polar and cross-polar fields vs. elevation angle for the patch antenna at the center frequency (1.02 GHz) in the *E*-plane. The MoM solution is shown by a solid curve; the Ansoft solution is given by a dashed curve.

The front-to-back ratio for the present patch antenna is small and the antenna is rather "omnidirectional" in every plane.

g. Near fields

It is desired to inspect the near field distributions in the antenna volume or on the antenna surface. The script `nearfield.m` finds and displays such distributions at a given frequency. In the case of the reduced-frequency PIFA the TM mode is not developed very well. The current on the metal surface (Fig. 4.23 top) is mostly concentrated around the loop formed by the feed and by the shorting stub. The excess charge (Fig. 4.23 bottom) is distributed along the patch nearly uniformly. The opposite charge is concentrated on the ground plane.

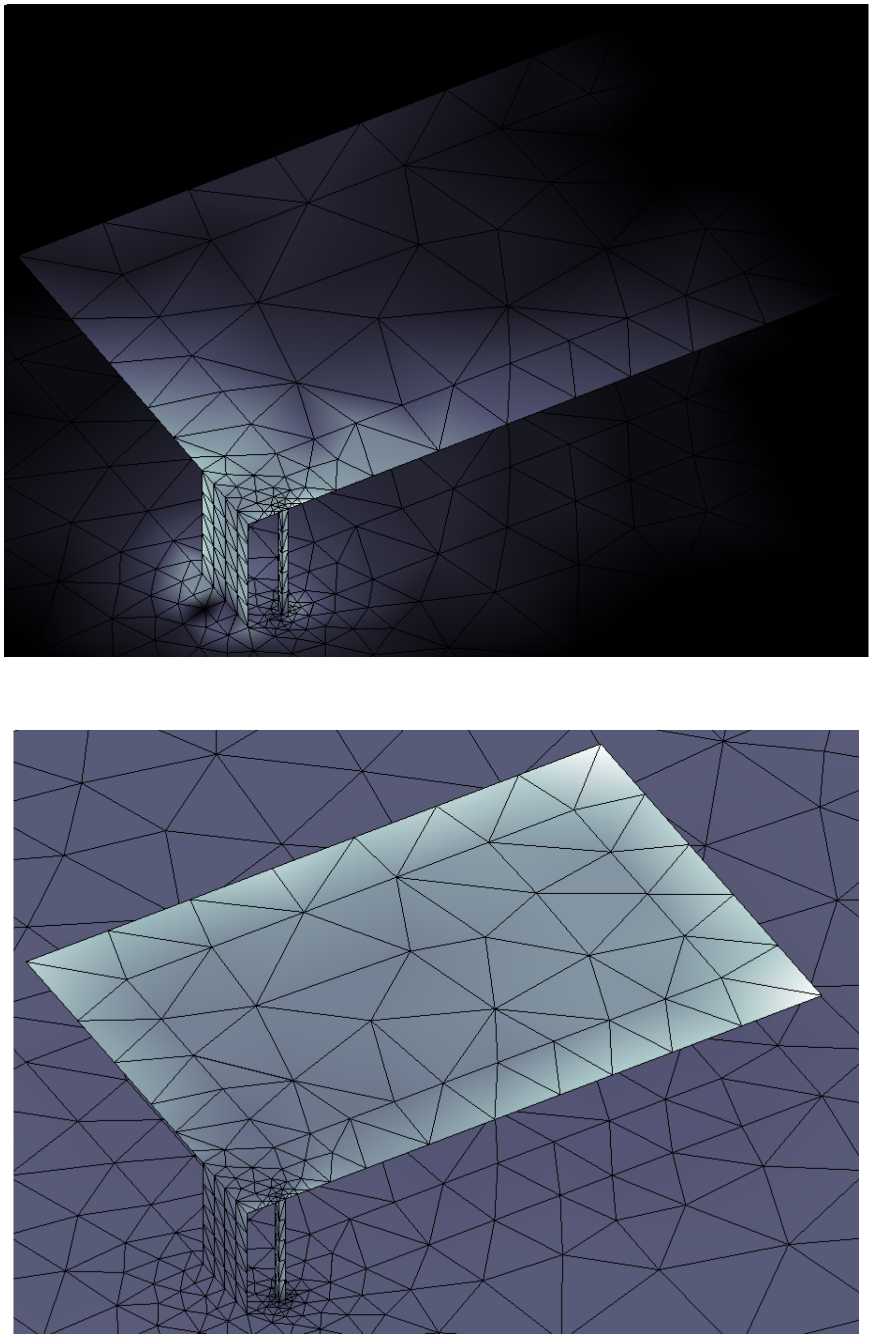

Fig. 4.23. Surface current distribution (top) and free charge distribution (bottom) on the metal surface at 1.02 GHz. Lighter colors correspond to larger current magnitudes.

References

1. C. A. Balanis, *Antenna Theory- Analysis and Design*, Wiley, New York, 2005, third edition.
2. K. Awadalla and T. Maclean, "Input impedance of a monopole antenna at the center of a finite ground plane," *IEEE Trans. Antennas and Propagation*, vol. AP-26, no. 2, pp. 244-248.
3. K. Awadalla and T. Maclean, "Monopole antenna at the center of circular ground plane," *IEEE Trans. Antennas and Propagation*, vol. AP-27, no. 2, pp. 151-153.
4. G. P. Junker, A. A. Kishk, and A. W. Glisson, "A novel delta gap source model for center fed cylindrical dipoles," *IEEE Trans. Antennas and Propagation*, vol. AP-43, no. 5, pp. 537-540, May 1995.
5. A. F. Gangi, S. Sensiper, and G. R. Dunn, "The characteristics of electrically short umbrella top loaded antennas," *IEEE Trans. Antennas and Propagation*, vol. AP-13, p. 864, 1965.
6. C. Y. Ying, "Theoretical study of finite dielectric-coated cylindrical antennas," *J. Math. Physics*, vol. 10, pp. 480-483, 1969.
7. M. A. Morgan and F. K. Schwering, "Eigenmode analysis of dielectric loaded top-hat monopole antennas**,**" *IEEE Trans. Antennas and Propagation*, vol. AP-42, no. 1, pp. 54-61, Jan. 1994.
8. L. A. Francavilla, J. S. McLean, H. D. Foltz, and G. F. Crook, "Mode-matching analysis of top-hat monopole antennas loaded with radially layered dielectric**,**" *IEEE Trans. Antennas and Propagation*, vol. AP-47, no. 1, pp. 179-185, Jan. 1999.
9. T. Taga, K. Tsunekawa, and A. Sasaki, "Antennas for detachable mobile radio units," *Review of the ECL, NTT*, Japan, vol. 35, no. 1, pp. 59-65, Jan. 1987.
10. T. Taga and K. Tsunekawa, "Performance Analysis of a Built-In Planar Inverted *F* Antenna for 800 MHz Band Portable Radio Units," *IEEE Journal on Selected Areas in Communications*, vol. 5, no. 5, pp. 921-929, Jun. 1987.
11. R. Bancroft, *Microstrip and Printed Antenna Design*, Noble Publishing, 2004, Atlanta, GA.

12. Kin-Lu Wong, *Compact and Broadband Microstrip Antennas*, Wiley, New York, 2002.
13. Li. Zhan and Y.Rahmat-Samii, "Optimization of PIFA-IFA combination in handset antenna designs," *IEEE Trans. Antennas and Propagation*, vol. AP-53, no. 5, pp. 1770-1778, May 2005.
14. R. Feik, H. Carrasco, M. Olmos, and H. D. Hristov, "PIFA input bandwidth enhancement by changing feed plate silhouette," *Electronics Letters*, vol. 40, no. 15, July 2004, pp. 921-922.